PHYSICAL REVIEW C **76**, 034001 (2007)

ΛNN and ΣNN systems at threshold. II. The effect of D waves

H. Garcilazo
Escuela Superior de Física y Matemáticas, Instituto Politécnico Nacional, Edificio 9, 07738 Mexico D.F., Mexico

A. Valcarce
Departamento de Física Fundamental, Universidad de Salamanca, E-37008 Salamanca, Spain

T. Fernández-Caramés
Departamento de Física Teórica e IFIC, Universidad de Valencia-CSIC, E-46100 Burjassot, Valencia, Spain
(Received 16 June 2007; published 4 September 2007)

Using the two-body interactions obtained from a chiral constituent quark model, we study all ΛNN and ΣNN states with $I = 0, 1, 2$ and $J = 1/2, 3/2$ at threshold, taking into account all three-body configurations with S and D wave components. We constrain further the limits for the ΛN spin-triplet scattering length $a_{1/2,1}$. Using the hypertriton binding energy, we find a narrow interval for the possible values of the ΛN spin-singlet scattering length $a_{1/2,0}$. We find that the ΣNN system has a quasibound state in the $(I, J) = (1, 1/2)$ channel very near threshold with a width of about 2.1 MeV.

DOI: 10.1103/PhysRevC.76.034001 PACS number(s): 13.75.Ev, 12.39.Jh, 21.45.+v

I. INTRODUCTION

The chiral constituent quark model has been very successful in the simultaneous description of the baryon-baryon interaction and the baryon spectrum as well as in the study of the two- and three-baryon bound-state problem for the nonstrange sector [1]. A simple generalization of this model to the strange sector has been applied to study the meson and baryon spectra [2] and the ΣNN bound-state problem [3]. Recently, a more elaborate description of the model was developed in Ref. [4], in which the ΛNN system was also studied.

In Ref. [4] we studied the ΛNN and ΣNN systems at threshold by solving the Faddeev equations of the coupled ΛNN-ΣNN system in the case of pure S wave configurations for the channels (I, J) with $I = 0, 1, 2$ and $J = 1/2, 3/2$. However, since the hyperon-nucleon and nucleon-nucleon interactions contain sizable tensor terms, there is a coupling between the $\ell = 0$ and $\ell = 2$ baryon-baryon channels and between the hyperon-nucleon-nucleon channels with $\ell = 0$ and $\lambda = 0$ to the channels with $\ell = 2$ and $\lambda = 2$. The importance of the tensor force at the two-body level manifests itself dramatically in the case of the $\Sigma^- p \to \Lambda n$ process which is dominated by the $\Sigma N(\ell = 0) \to \Lambda N(\ell = 2)$ transition such that if one includes only the $\Sigma N(\ell = 0) \to \Lambda N(\ell = 0)$ transition it is practically impossible to describe the cross section [3] (this problem was first observed in Ref. [5]). Thus, one expects that also at the three-body level the effect of the D waves will be important.

In Refs. [3,4] we considered all configurations in which the baryon-baryon subsystems are in an S wave and the third particle is also in an S wave with respect to the pair. However, to construct the two-body t matrices that serve as input to the Faddeev equations, we considered the full interaction including the contribution of the D waves and of course the coupling between the ΣN and ΛN subsystems (which is known as the truncated t-matrix approximation [6]). In Ref. [4] we found that our model with only S waves is able to predict correctly the binding energy of the hypertriton, which is a bound state in the channel $(I, J) = (0, 1/2)$. We also found that the channel $(I, J) = (0, 3/2)$ will develop a bound state if the triplet ΛN scattering length $a_{1/2,1}$ is larger than 1.68 fm. In the case of the ΣNN system, the channel $(I, J) = (1, 1/2)$ develops a quasibound state in some cases, while the channel $(I, J) = (0, 1/2)$ is also attractive but unbound.

In this work, we will further pursue the study of the ΛNN-ΣNN system at threshold in which the three-body D wave components are considered. We will analyze their effects by comparing our results with those obtained when using only three-body S wave contributions. The structure of the paper is the following. In the next section we will resume the basic aspects of the two-body interactions and present the generalization of the Faddeev equations of Ref. [4] for arbitrary orbital angular momenta. In Sec. III we will present our results, comparing them to those of Ref. [4] to discuss the effect of the three-body D waves. Finally, in Sec. IV we summarize our main conclusions.

II. FORMALISM

A. Two-body interactions

The baryon-baryon interactions involved in the study of the coupled ΣNN-ΛNN system are obtained from the chiral constituent quark model [1,2]. In this model, baryons are described as clusters of three interacting massive (constituent) quarks, the mass coming from the spontaneous breaking of chiral symmetry. The first ingredient of the quark-quark interaction is a confining potential (CON). Perturbative aspects of QCD are taken into account by means of a one-gluon potential (OGE). Spontaneous breaking of chiral symmetry gives rise to boson exchanges between quarks. In particular, there appear pseudoscalar boson exchanges and their corresponding scalar partners [4]. Thus, the quark-quark interaction will read

$$V_{qq}(\vec{r}_{ij}) = V_{\rm CON}(\vec{r}_{ij}) + V_{\rm OGE}(\vec{r}_{ij}) + V_{\chi}(\vec{r}_{ij}) + V_{S}(\vec{r}_{ij}), \quad (1)$$

where the i and j indices are associated with i and j quarks, respectively, and $\vec{r}_{ij}$ stands for the interquark distance. V_χ denotes the pseudoscalar meson-exchange interaction discussed in Ref. [3], and V_S stands for the scalar meson-exchange potential described in Ref. [4]. Explicit expressions of all the interacting potentials and a more detailed discussion of the model can be found in Refs. [2,4]. To derive the local $B_1B_2 \to B_3B_4$ potentials from the basic qq interaction defined above, we use a Born-Oppenheimer approximation. Explicitly, the potential is calculated as

$$V_{B_1B_2(LST)\to B_3B_4(L'S'T)}(R) = \xi_{LST}^{L'S'T}(R) - \xi_{LST}^{L'S'T}(\infty), \tag{2}$$

where

$$\xi_{LST}^{L'S'T}(R) = \frac{\left\langle \Psi_{B_3B_4}^{L'S'T}(\vec{R}) \right| \sum_{i<j=1}^{6} V_{qq}(\vec{r}_{ij}) \left| \Psi_{B_1B_2}^{LST}(\vec{R}) \right\rangle}{\sqrt{\left\langle \Psi_{B_3B_4}^{L'S'T}(\vec{R}) \middle| \Psi_{B_3B_4}^{L'S'T}(\vec{R}) \right\rangle}\sqrt{\left\langle \Psi_{B_1B_2}^{LST}(\vec{R}) \middle| \Psi_{B_1B_2}^{LST}(\vec{R}) \right\rangle}}. \tag{3}$$

In the last expression, the quark coordinates are integrated out, keeping R fixed; the resulting interaction is a function of the B_i–B_j relative distance. The wave function $\Psi_{B_iB_j}^{LST}(\vec{R})$ for the two-baryon system is discussed in detail in Ref. [1].

B. Faddeev equations at threshold

Our method [3] for transforming the Faddeev equations from integral equations in two continuous variables into integral equations in just one continuous variable is based in the expansion of the two-body t matrices

$$t_i(p_i, p_i'; e) = \sum_{nr} P_n(x_i)\tau_i^{nr}(e)P_r(x_i'), \tag{4}$$

where P_n and P_r are Legendre polynomials,

$$x_i = \frac{p_i - b}{p_i + b}, \tag{5}$$

$$x_i' = \frac{p_i' - b}{p_i' + b}, \tag{6}$$

and p_i and p_i' are the initial and final relative momenta of the pair jk, while b is a scale parameter on which the results do not depend.

In Ref. [4] we give the integral equations for βd scattering at threshold with $\beta = \Sigma$ or Λ including the full coupling between ΛNN and ΣNN states for the case of pure S wave configurations, assuming that particle 1 is the hyperon and particles 2 and 3 are the two nucleons. To include arbitrary orbital angular momentum configurations, we consider the total angular momentum and total isospin J and I, while σ_1 (τ_1) and σ_3 (τ_3) stand for the spin (isospin) of the hyperon and the nucleon, respectively. In addition, ℓ_i, s_i, j_i, i_i, λ_i, and J_i are the orbital angular momentum, spin, total angular momentum, and isospin of the pair jk, while λ_i is the orbital angular momentum between particle i and the pair jk, and J_i is the result of coupling λ_i and σ_i. If in Eqs. (10)–(14) of Ref. [4] we make the replacements

$$\{ns_2i_2\} \to \{n\ell_2s_2j_2i_2\lambda_2J_2\} \equiv \gamma_2, \tag{7}$$

$$\{ms_3i_3\} \to \{m\ell_3s_3j_3i_3\lambda_3J_3\} \equiv \gamma_3, \tag{8}$$

$$\{rs_1i_1\} \to \{r\ell_1s_1j_1i_1\lambda_1J_1\} \equiv \gamma_1, \tag{9}$$

the three-body equations become

$$\begin{aligned} T_{2;JI;\beta}^{\gamma_2}(q_2) &= B_{2;JI;\beta}^{\gamma_2}(q_2) + \sum_{\gamma_3}\int_0^\infty dq_3 \\ &\quad \times \Bigg[(-1)^{1+\ell_2+\sigma_1+\sigma_3-s_2+\tau_1+\tau_3-i_2}A_{23;JI}^{\gamma_2\gamma_3}(q_2,q_3;E) \\ &\quad + 2\sum_{\gamma_1}\int_0^\infty dq_1 A_{31;JI}^{\gamma_2\gamma_1}(q_2,q_1;E) \\ &\quad \times A_{13;JI}^{\gamma_1\gamma_3}(q_1,q_3;E)\Bigg] T_{2;JI;\beta}^{\gamma_3}(q_3), \end{aligned} \tag{10}$$

where $T_{2;JI;\beta}^{\gamma_2}(q_2)$ is a two-component vector

$$T_{2;JI;\beta}^{\gamma_2}(q_2) = \begin{pmatrix} T_{2;JI;\Sigma\beta}^{\gamma_2}(q_2) \\ T_{2;JI;\Lambda\beta}^{\gamma_2}(q_2) \end{pmatrix}, \tag{11}$$

while the kernel of Eq. (10) is a 2×2 matrix defined by

$$A_{23;JI}^{\gamma_2\gamma_3}(q_2,q_3;E) = \begin{pmatrix} A_{23;JI;\Sigma\Sigma}^{\gamma_2\gamma_3}(q_2,q_3;E) & A_{23;JI;\Sigma\Lambda}^{\gamma_2\gamma_3}(q_2,q_3;E) \\ A_{23;JI;\Lambda\Sigma}^{\gamma_2\gamma_3}(q_2,q_3;E) & A_{23;JI;\Lambda\Lambda}^{\gamma_2\gamma_3}(q_2,q_3;E) \end{pmatrix}, \tag{12}$$

$$A_{31;JI}^{\gamma_2\gamma_1}(q_2,q_1;E) = \begin{pmatrix} A_{31;JI;\Sigma N(\Sigma)}^{\gamma_2\gamma_1}(q_2,q_1;E) & A_{31;JI;\Sigma N(\Lambda)}^{\gamma_2\gamma_1}(q_2,q_1;E) \\ A_{31;JI;\Lambda N(\Sigma)}^{\gamma_2\gamma_1}(q_2,q_1;E) & A_{31;JI;\Lambda N(\Lambda)}^{\gamma_2\gamma_1}(q_2,q_1;E) \end{pmatrix}, \tag{13}$$

$$A_{13;JI}^{\gamma_1\gamma_3}(q_1,q_3;E) = \begin{pmatrix} A_{13;JI;N\Sigma}^{\gamma_1\gamma_3}(q_1,q_3;E) & 0 \\ 0 & A_{13;JI;N\Lambda}^{\gamma_1\gamma_3}(q_1,q_3;E) \end{pmatrix}, \tag{14}$$

where

$$\begin{aligned} A_{23;JI;\alpha\beta}^{\gamma_2\gamma_3}(q_2,q_3;E) &= \sum_{\ell_2'r}\tau_{2;\ell_2\ell_2's_2j_2i_2;\alpha\beta}^{nr}\left(E - \frac{q_2^2}{2\nu_2}\right)\frac{q_3^2}{2}\int_{-1}^{1} d\cos\theta \\ &\quad \times \frac{P_r(x_2')D_{23;JI;\beta}^{\rho_2'\rho_3}(q_2,q_3,\cos\theta)P_m(x_3)}{E + \Delta E\delta_{\beta\Lambda} - p_3^2/2\mu_3 - q_3^2/2\nu_3 + i\epsilon}; \\ &\quad \alpha,\beta = \Sigma,\Lambda, \end{aligned} \tag{15}$$

$$\begin{aligned} A_{31;JI;\alpha N(\beta)}^{\gamma_2\gamma_1}(q_2,q_1;E) &= \sum_{\ell_2'r}\tau_{3;\ell_2\ell_2's_2j_2i_2;\alpha\beta}^{nr}\left(E - \frac{q_2^2}{2\nu_2}\right)\frac{q_1^2}{2}\int_{-1}^{1} d\cos\theta \\ &\quad \times \frac{P_r(x_3')D_{31;JI;\beta}^{\rho_2'\rho_1}(q_2,q_1,\cos\theta)P_m(x_1)}{E + \Delta E\delta_{\beta\Lambda} - p_1^2/2\mu_1 - q_1^2/2\nu_1 + i\epsilon}; \\ &\quad \alpha,\beta = \Sigma,\Lambda, \end{aligned} \tag{16}$$

$$
\begin{aligned}
&A^{\gamma_1\gamma_3}_{13;JI;N\beta}(q_1, q_3; E) \\
&\quad = \sum_{\ell_1' r} \tau^{nr}_{1;\ell_1\ell_1' s_1 j_1 i_1;NN}\left(E + \Delta E\delta_{\beta\Lambda} - \frac{q_1^2}{2\nu_1}\right)\frac{q_3^2}{2} \\
&\quad\quad \times \int_{-1}^{1} d\cos\theta \frac{P_r(x_1')D^{\rho_1'\rho_3}_{13;JI;\beta}(q_1, q_3, \cos\theta)P_m(x_3)}{E+\Delta E\delta_{\beta\Lambda}-p_3^2/2\mu_3-q_3^2/2\nu_3.+i\epsilon}; \\
&\quad\quad \beta = \Sigma, \Lambda,
\end{aligned} \tag{17}
$$

where

$$\rho_i \equiv \{\ell_i s_i j_i i_i \lambda_i J_i\}, \tag{18}$$

$$\rho_i' \equiv \{\ell_i' s_i j_i i_i \lambda_i J_i\}, \tag{19}$$

and η_i and ν_i are the usual reduced masses

$$
\begin{aligned}
\eta_i &= \frac{m_j m_k}{m_j + m_k}, \\
\nu_i &= \frac{m_i(m_j + m_k)}{m_i + m_j + m_k}.
\end{aligned} \tag{20}
$$

In Eqs. (15)–(20) the isospin and mass of particle 1 (the hyperon) is determined by the subindex β. The subindex $\alpha N(\beta)$ in Eq. (16) indicates a transition $\alpha N \to \beta N$ with a nucleon as spectator followed by a $NN \to NN$ transition with β as spectator. The angular momentum functions $D^{\rho_i\rho_j}_{ij;JI;\beta}(q_i, q_j, \cos\theta)$ are given by

$$
\begin{aligned}
&D^{\rho_i\rho_j}_{ij;JI;\beta}(q_i, q_j, \cos\theta) \\
&\quad = (-)^{i_j+\tau_j-I}\sqrt{(2i_i+1)(2i_j+1)}W(\tau_j\tau_k I\tau_i; i_i i_j) \\
&\quad\quad \times\sqrt{(2j_i+1)(2j_j+1)(2J_i+1)(2J_j+1)} \\
&\quad\quad \times\sum_{LS}(2L+1)(2S+1)\begin{Bmatrix} \ell_i & \lambda_i & L \\ s_i & \sigma_i & S \\ j_i & J_i & J\end{Bmatrix}\begin{Bmatrix} \ell_j & \lambda_j & L \\ s_j & \sigma_j & S \\ j_j & J_j & J\end{Bmatrix} \\
&\quad\quad \times(-)^{s_j+\sigma_j-S}\sqrt{(2s_i+1)(2s_j+1)}W(\sigma_j\sigma_k S\sigma_i; s_i s_j) \\
&\quad\quad \times\frac{1}{2L+1}\sum_{M m_i m_j} C^{\ell_i\lambda_i L}_{m_i, M-m_i, M} C^{\ell_j\lambda_j L}_{m_j, M-m_j, M}\Gamma_{\ell_i m_i}\Gamma_{\lambda_i M-m_i} \\
&\quad\quad \times\Gamma_{\ell_j m_j}\Gamma_{\lambda_j M-m_j}\cos(-M\theta - m_i\theta_i + m_j\theta_j),
\end{aligned} \tag{21}
$$

where W is the Racah coefficient, and $\Gamma_{\ell m} = 0$ if $\ell - m$ is odd, while

$$\Gamma_{\ell m} = \frac{(-)^{(\ell+m)/2}\sqrt{(2\ell+1)(\ell+m)!(\ell-m)!}}{2^\ell((\ell+m)/2)!((\ell-m)/2)!} \tag{22}$$

if $\ell - m$ is even. The angles θ, θ_i, and θ_j are given by

$$\cos\theta = \frac{\vec{q}_i\cdot\vec{q}_j}{q_i q_j}, \tag{23}$$

$$\cos\theta_i = \frac{\vec{q}_i\cdot\vec{p}_i}{q_i p_i}, \tag{24}$$

$$\cos\theta_j = \frac{\vec{q}_j\cdot\vec{p}_j}{q_j p_j}, \tag{25}$$

with

$$
\begin{aligned}
\vec{p}_i &= -\vec{q}_j - \frac{\eta_i}{m_k}\vec{q}_i, \\
\vec{p}_j &= \vec{q}_i + \frac{\eta_j}{m_k}\vec{q}_j.
\end{aligned} \tag{26}
$$

$\tau^{nr}_{i;\ell_i\ell_i' s_i j_i i_i;\alpha\beta}(e)$ are the coefficients of the expansion in terms of Legendre polynomials of the hyperon-nucleon t matrix $t_{i;\ell_i\ell_i' s_i j_i i_i;\alpha\beta}(p_i, p_i'; e)$ for the transition $\alpha N \to \beta N$, i.e.,

$$
\begin{aligned}
\tau^{nr}_{i;\ell_i\ell_i' s_i j_i i_i;\alpha\beta}(e) &= \frac{2n+1}{2}\frac{2r+1}{2} \\
&\quad \times\int_{-1}^{1} dx_i\int_{-1}^{1} dx_i' P_n(x_i)t_{i;\ell_i\ell_i' s_i j_i i_i;\alpha\beta}(p_i, p_i'; e)P_r(x_i').
\end{aligned} \tag{27}
$$

The energy shift ΔE is chosen such that at the βd threshold, the momentum of the αd system has the correct value, i.e.,

$$\Delta E = \frac{[(m_\beta+m_d)^2-(m_\alpha+m_d)^2][(m_\beta+m_d)^2-(m_\alpha-m_d)^2]}{8\mu_{\alpha d}(m_\beta+m_d)^2}, \tag{28}$$

where $\mu_{\alpha d}$ is the αd reduced mass.

The inhomogeneous term of Eq. (10), $B^{\gamma_2}_{2;JI;\beta}(q_2)$, is a two-component vector

$$B^{\gamma_2}_{2;JI;\beta}(q_2) = \begin{pmatrix} B^{\gamma_2}_{2;JI;\Sigma\beta}(q_2) \\ B^{\gamma_2}_{2;JI;\Lambda\beta}(q_2)\end{pmatrix}, \tag{29}$$

where

$$
\begin{aligned}
B^{\gamma_2}_{2;JI;\alpha\beta}(q_2) &= \sum_{\ell_2' r\rho_{10}} \tau^{nr}_{2;\ell_2\ell_2' s_2 j_2 i_2;\alpha\beta}\left(E^{\rm th}_\beta - q_2^2/2\nu_2\right) \\
&\quad \times P_r(x_2')D^{\rho_2'\rho_{10}}_{31;JI;\beta}(q_2, 0, 0)\phi_{d;l_1}(q_2),
\end{aligned} \tag{30}
$$

and

$$\rho_{10} \equiv \{\ell_1, s_1 = 1, j_1 = 1, i_1 = 0, \lambda_1 = 0, J_1\}, \tag{31}$$

which corresponds to a hyperon-deuteron initial state, $\phi_{d;\ell_1}(q_2)$ is the deuteron wave function with orbital angular momentum ℓ_1, $E^{\rm th}_\beta$ is the energy of the βd threshold, $P_r(x_2')$ is a Legendre polynomial of order r, and

$$x_2' = \frac{\frac{\eta_2}{m_3}q_2 - b}{\frac{\eta_2}{m_3}q_2 + b}. \tag{32}$$

Finally, after solving the inhomogeneous set of equations (10), the βd scattering length is given by

$$A_{\beta d} = -\pi\mu_{\beta d}T_{\beta\beta}, \tag{33}$$

with

$$
\begin{aligned}
T_{\beta\beta} &= 2\sum_{n\rho_{10}\rho_2}\int_0^\infty q_2^2 dq_2\phi_{d;\ell_1}(q_2)P_n(x_2') \\
&\quad \times D^{\rho_{10}\rho_2}_{13;JI;\beta}(0, q_2, 0)T^{\gamma_2}_{2;JI;\beta\beta}(q_2).
\end{aligned} \tag{34}
$$

In the case of the ΣNN system, even for energies below the Σd threshold, one encounters the three-body singularities of the ΛNN system so that to solve the integral equations (10), one has to use the contour rotation method in which the momenta are rotated into the complex plane $q_i \to q_i e^{-i\phi}$, since as pointed out in Ref. [3] the results do not depend on the contour rotation angle ϕ.

We give in Table I the two-body channels that contribute in the case of the six three-body channels (I, J) with $I = 0, 1, 2$ and $J = 1/2, 3/2$. For the parameter b in Eqs. (5) and (6) we found that $b = 3$ fm^{-1} leads to very stable results, while for

TABLE I. Two-body ΣN channels with a nucleon as spectator $(\ell_\Sigma s_\Sigma j_\Sigma i_\Sigma \lambda_\Sigma J_\Sigma)_N$, two-body ΛN channels with a nucleon as spectator $(\ell_\Lambda s_\Lambda j_\Lambda i_\Lambda \lambda_\Lambda J_\Lambda)_N$, two-body NN channels with a Σ as spectator $(\ell_N s_N j_N i_N \lambda_N J_N)_\Sigma$, and two-body NN channels with a Λ as spectator $(\ell_N s_N j_N i_N \lambda_N J_N)_\Lambda$ that contribute to a given ΣNN-ΛNN state with total isospin I and total angular momentum J.

I	J	$(\ell_\Sigma s_\Sigma j_\Sigma i_\Sigma \lambda_\Sigma J_\Sigma)_N$	$(\ell_\Lambda s_\Lambda j_\Lambda i_\Lambda \lambda_\Lambda J_\Lambda)_N$	$(\ell_N s_N j_N i_N \lambda_N J_N)_\Sigma$	$(\ell_N s_N j_N i_N \lambda_N J_N)_\Lambda$
0	$\frac{1}{2}$	$(000\frac{1}{2}0\frac{1}{2}),(011\frac{1}{2}0\frac{1}{2}),(211\frac{1}{2}0\frac{1}{2}),(011\frac{1}{2}2\frac{3}{2}),(211\frac{1}{2}2\frac{3}{2})$	$(000\frac{1}{2}0\frac{1}{2}),(011\frac{1}{2}0\frac{1}{2}),(211\frac{1}{2}0\frac{1}{2}),(011\frac{1}{2}2\frac{3}{2}),(211\frac{1}{2}2\frac{3}{2})$	$(00010\frac{1}{2})$	$(01100\frac{1}{2}),(21100\frac{1}{2}),(01102\frac{3}{2}),(21102\frac{3}{2})$
1	$\frac{1}{2}$	$(000\frac{1}{2}0\frac{1}{2}),(011\frac{1}{2}0\frac{1}{2}),(211\frac{1}{2}0\frac{1}{2}),(011\frac{1}{2}2\frac{3}{2}),(211\frac{1}{2}2\frac{3}{2}),(000\frac{3}{2}0\frac{1}{2}),(011\frac{3}{2}0\frac{1}{2}),(211\frac{3}{2}0\frac{1}{2}),(011\frac{3}{2}2\frac{3}{2}),(211\frac{3}{2}2\frac{3}{2})$	$(000\frac{1}{2}0\frac{1}{2}),(011\frac{1}{2}0\frac{1}{2}),(211\frac{1}{2}0\frac{1}{2}),(011\frac{1}{2}2\frac{3}{2}),(211\frac{1}{2}2\frac{3}{2})$	$(00010\frac{1}{2}),(01100\frac{1}{2}),(21100\frac{1}{2}),(01102\frac{3}{2}),(21102\frac{3}{2})$	$(00010\frac{1}{2})$
2	$\frac{1}{2}$	$(000\frac{3}{2}0\frac{1}{2}),(011\frac{3}{2}0\frac{1}{2}),(211\frac{3}{2}0\frac{1}{2}),(011\frac{3}{2}2\frac{3}{2}),(211\frac{3}{2}2\frac{3}{2})$		$(00010\frac{1}{2})$	
0	$\frac{3}{2}$	$(000\frac{1}{2}2\frac{3}{2}),(011\frac{1}{2}0\frac{1}{2}),(211\frac{1}{2}0\frac{1}{2}),(011\frac{1}{2}2\frac{3}{2}),(011\frac{1}{2}2\frac{5}{2}),(211\frac{1}{2}2\frac{3}{2}),(211\frac{1}{2}2\frac{5}{2})$	$(000\frac{1}{2}2\frac{3}{2}),(011\frac{1}{2}0\frac{1}{2}),(211\frac{1}{2}0\frac{1}{2}),(011\frac{1}{2}2\frac{3}{2}),(011\frac{1}{2}2\frac{5}{2}),(211\frac{1}{2}2\frac{3}{2}),(211\frac{1}{2}2\frac{5}{2})$	$(00012\frac{3}{2})$	$(01100\frac{1}{2}),(21100\frac{1}{2}),(01102\frac{3}{2}),(01102\frac{5}{2}),(21102\frac{3}{2}),(21102\frac{5}{2})$
1	$\frac{3}{2}$	$(000\frac{1}{2}2\frac{3}{2}),(011\frac{1}{2}0\frac{1}{2}),(211\frac{1}{2}0\frac{1}{2}),(011\frac{1}{2}2\frac{3}{2}),(011\frac{1}{2}2\frac{5}{2}),(211\frac{1}{2}2\frac{3}{2}),(211\frac{1}{2}2\frac{5}{2}),(000\frac{3}{2}2\frac{3}{2}),(011\frac{3}{2}0\frac{1}{2}),(211\frac{3}{2}0\frac{1}{2}),(011\frac{3}{2}2\frac{3}{2}),(011\frac{3}{2}2\frac{5}{2}),(211\frac{3}{2}2\frac{3}{2}),(211\frac{3}{2}2\frac{5}{2})$	$(000\frac{1}{2}2\frac{3}{2}),(011\frac{1}{2}0\frac{1}{2}),(211\frac{1}{2}0\frac{1}{2}),(011\frac{1}{2}2\frac{3}{2}),(011\frac{1}{2}2\frac{5}{2}),(211\frac{1}{2}2\frac{3}{2}),(211\frac{1}{2}2\frac{5}{2})$	$(00012\frac{3}{2}),(01100\frac{1}{2}),(21100\frac{1}{2}),(01102\frac{3}{2}),(01102\frac{5}{2}),(21102\frac{3}{2}),(21102\frac{5}{2})$	$(00012\frac{3}{2})$
2	$\frac{3}{2}$	$(000\frac{3}{2}2\frac{3}{2}),(011\frac{3}{2}0\frac{1}{2}),(211\frac{3}{2}0\frac{1}{2}),(011\frac{3}{2}2\frac{3}{2}),(011\frac{3}{2}2\frac{5}{2}),(211\frac{3}{2}2\frac{3}{2}),(211\frac{3}{2}2\frac{5}{2})$		$(00012\frac{3}{2})$	

the expansion (4) we took twelve Legendre polynomials, i.e., $0 \leqslant n \leqslant 11$.

III. RESULTS

In Ref. [4] we constructed different families of interacting potentials, by introducing small variations of the mass of the effective scalar exchange potentials, that allow us to study the dependence of the results on the strength of the spin-singlet and spin-triplet hyperon-nucleon interactions. These potentials are characterized by the ΛN scattering lengths $a_{i,s}$, and they reproduce the cross sections near threshold of the five hyperon-nucleon processes for which data are available (see Ref. [4]).

A. ΛNN system

The channels $(I, J) = (0,1/2)$ and $(0,3/2)$ are the most attractive ones of the ΛNN system. In particular, the channel (0,1/2) has the only bound state of this system, the hypertriton. We give in Table II the results of the models constructed in Ref. [4] for the two Λd scattering lengths and the

TABLE II. Λd scattering lengths $A_{0,3/2}$ and $A_{0,1/2}$ (in fm) and hypertriton binding energy $B_{0,1/2}$ (in MeV) for several hyperon-nucleon interactions characterized by ΛN scattering lengths $a_{1/2,0}$ and $a_{1/2,1}$ (in fm). We give in parentheses the results obtained in Ref. [4] including only three-body S wave configurations.

$a_{1/2,0}$	$a_{1/2,1}$	$A_{0,3/2}$	$A_{0,1/2}$	$B_{0,1/2}$
2.48	1.41	31.9 (66.3)	−16.0 (−20.0)	0.129 (0.089)
2.48	1.65	−72.8 (198.2)	−13.8 (−17.2)	0.178 (0.124)
2.48	1.72	−40.8 (−179.8)	−13.3 (−16.6)	0.192 (0.134)
2.48	1.79	−28.5 (−62.7)	−12.9 (−16.0)	0.207 (0.145)
2.48	1.87	−22.0 (−38.2)	−12.5 (−15.4)	0.223 (0.156)
2.48	1.95	−17.9 (−27.6)	−12.1 (−14.9)	0.239 (0.168)
2.31	1.65	−76.0 (198.2)	−17.1 (−22.4)	0.113 (0.070)
2.55	1.65	−73.6 (198.2)	−13.6 (−16.8)	0.185 (0.130)
2.74	1.65	−72.1 (198.2)	−12.0 (−14.4)	0.244 (0.182)

hypertriton binding energy. We compare them with the results, in parentheses, obtained in Ref. [4] when only the three-body S wave configurations were included. As a consequence of considering the D waves, the hypertriton binding energy increases by about 50–60 keV [7], while the $A_{0,1/2}$ scattering length decreases by about 3–5 fm. The largest changes occur in the $A_{0,3/2}$ scattering length where both positive and negative values appeared, which means, in the case of the negative values, that a bound state is generated in the $(I, J) = (0, 3/2)$ channel. Since this channel depends mainly on the spin-triplet hyperon-nucleon interaction and experimentally there is no evidence whatsoever for the existence of a $(I, J) = (0, 3/2)$ bound state, one can use the results of this channel to set limits on the value of the hyperon-nucleon spin-triplet scattering length $a_{1/2,1}$. We plot in Fig. 1 the inverse of the two Λd scattering lengths as a function of the spin-triplet ΛN scattering length $a_{1/2,1}$. As one can see, by increasing $a_{1/2,1}$, one increases the amount of attraction that is present in the system, since the three-body channel $(I, J) = (0, 3/2)$ becomes bound if $a_{1/2,1} > 1.58$ fm. Moreover, we found in Ref. [4] that the fit of the hyperon-nucleon cross sections is worsened when the spin-triplet ΛN scattering length is smaller than 1.41 fm; so we conclude that $1.41 \leqslant a_{1/2,1} \leqslant 1.58$ fm. This range of values is narrower than the one found in Ref. [4].

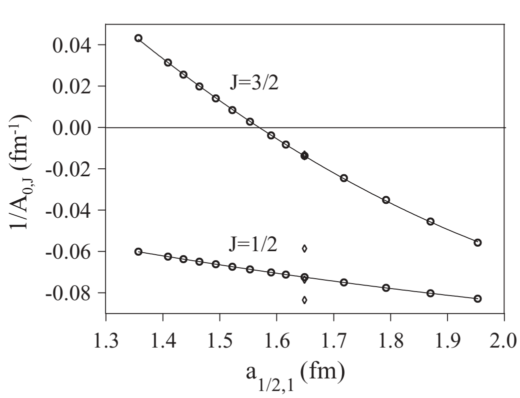

FIG. 1. Inverse of the $(I, J) = (0, 1/2)$ and $(0, 3/2)$ Λd scattering lengths as a function of the ΛN $a_{1/2,1}$ scattering length.

TABLE III. Hypertriton binding energy (in MeV) for several hyperon-nucleon interactions characterized by ΛN scattering lengths $a_{1/2,0}$ and $a_{1/2,1}$ (in fm) which are within the experimental error bars $B_{0,1/2} = 0.130 \pm 0.050$ MeV.

	$a_{1/2,1}$=1.41	$a_{1/2,1}$=1.46	$a_{1/2,1}$=1.52	$a_{1/2,1}$=1.58
$a_{1/2,0}$=2.33	0.080	0.087	0.096	0.106
$a_{1/2,0}$=2.39	0.094	0.102	0.112	0.122
$a_{1/2,0}$=2.48	0.129	0.140	0.152	0.164

To show the dependence of these results on the spin-singlet ΛN scattering length $a_{1/2,0}$, we have also plotted in Fig. 1 the results of the last three rows of Table II where $a_{1/2,1} = 1.65$ fm and $a_{1/2,0} = 2.31$, 2.55, and 2.74 fm (they are denoted by *diamonds*). As one can see, $1/A_{0,3/2}$ almost does not change, although there is a large sensitivity in $1/A_{0,1/2}$. To try to set some limits to the hyperon-nucleon spin-singlet scattering length, we have calculated in Table III the hypertriton binding energy, using for the hyperon-nucleon spin-triplet scattering length the allowed values $1.41 \leqslant a_{1/2,1} \leqslant 1.58$ fm and using for the spin-singlet scattering length $2.33 \leqslant a_{1/2,0} \leqslant 2.48$ fm, which leads to results for the hypertriton binding energy within the experimental error bars $B_{0,1/2} = 0.13 \pm 0.05$ MeV.

With regard to the isospin 1 channels $(I, J) = (1, 1/2)$ and (1,3/2), we show in Fig. 2 the Fredholm determinant of these channels for energies below the ΛNN threshold, where one sees that the (1, 1/2) channel is attractive but not enough to produce a bound state, while the (1, 3/2) channel is repulsive. These results are very similar to those found in Ref. [4].

B. ΣNN system

We show in Table IV the Σd scattering lengths $A'_{1,3/2}$ and $A'_{1,1/2}$. The Σd scattering lengths are complex since the inelastic ΛNN channels are always open. The scattering length $A'_{1,3/2}$ depends mainly on the spin-triplet hyperon-nucleon

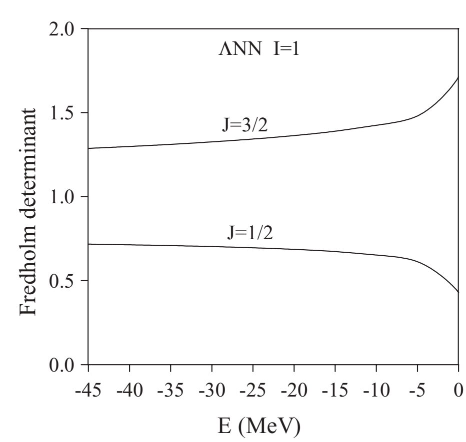

FIG. 2. Fredholm determinant for the ΛNN channels $(I, J) = (1, 1/2)$ and $(1, 3/2)$ for the model with $a_{1/2,0} = 2.48$ and $a_{1/2,1} = 1.41$ fm and energies below the ΛNN threshold.

TABLE IV. Σd scattering lengths $A'_{1,3/2}$ and $A'_{1,1/2}$ (in fm) and position of the quasibound state $B'_{1,1/2}$ (in MeV) for several hyperon-nucleon interactions characterized by ΛN scattering lengths $a_{1/2,0}$ and $a_{1/2,1}$ (in fm). We give in parentheses the results obtained in Ref. [4] with only three-body S waves.

$a_{1/2,0}$	$a_{1/2,1}$	$A'_{1,3/2}$	$A'_{1,1/2}$	$B'_{1,1/2}$
2.48	1.41	$0.14 + i0.24$ $(0.20 + i0.26)$	$19.82 + i16.94$ $(19.28 + i25.37)$	$2.92 - i2.17$
2.48	1.65	$0.28 + i0.27$ $(0.36 + i0.29)$	$12.08 + i38.98$ $(-1.55 + i42.31)$	$2.84 - i2.14$
2.48	1.72	$0.32 + i0.28$ $(0.40 + i0.30)$	$2.92 + i43.20$ $(-10.47 + i40.25)$	$2.82 - i2.11$
2.48	1.79	$0.36 + i0.29$ $(0.44 + i0.31)$	$-8.00 + i42.58$ $(-17.33 + i35.01)$	$2.79 - i2.10$
2.48	1.87	$0.40 + i0.30$ $(0.49 + i0.33)$	$-16.90 + i37.08$ $(-21.16 + i28.54)$	$2.77 - i2.09$
2.48	1.95	$0.45 + i0.31$ $(0.54 + i0.34)$	$-21.73 + i29.48$ $(-22.44 + i22.44)$	$2.75 - i2.08$
2.31	1.65	$0.28 + i0.27$ $(0.36 + i0.29)$	$19.01 + i23.21$ $(14.95 + i31.61)$	$2.88 - i2.14$
2.55	1.65	$0.28 + i0.27$ $(0.36 + i0.29)$	$-12.81 + i43.49$ $(-21.04 + i33.19)$	$2.79 - i2.11$
2.74	1.65	$0.28 + i0.27$ $(0.36 + i0.29)$	$-26.01 + i17.95$ $(-23.29 + i13.32)$	$2.73 - i2.09$

channels, and both its real and imaginary parts increase when the spin-triplet hyperon-nucleon scattering length increases. The effect of the three-body D waves is to lower the real part by about 20% and the imaginary part by about 10%. The scattering length $A'_{1,1/2}$ shows large variations between the results with and without three-body D waves, but this is due, as we will see next, to the fact that there is a pole very near threshold, a situation quite similar to that of the $A_{0,3/2}$ Λd scattering length discussed in the previous subsection.

We plot in Fig. 3 the real and imaginary parts of the Σd scattering length $A'_{1,1/2}$ as functions of the spin-triplet ΛN scattering length $a_{1/2,1}$, since by increasing $a_{1/2,1}$ one is increasing the amount of attraction that is present in the three-body channel. As one can see, $\mathrm{Re}(A'_{1,1/2})$ changes sign going from positive to negative, while at the same time $\mathrm{Im}(A'_{1,1/2})$ has a maximum. These two features are the typical ones that signal that the channel has a quasibound state [8]. Since in the case of the ΣNN system we are using the contour rotation method, which opens large portions of the second Riemann sheet, we can search for the position of this pole in the complex plane, which is given in the last column of Table IV. As one can see, the position of the pole changes very little with the model used to calculate it, and it lies at around 2.8–i2.1 MeV.

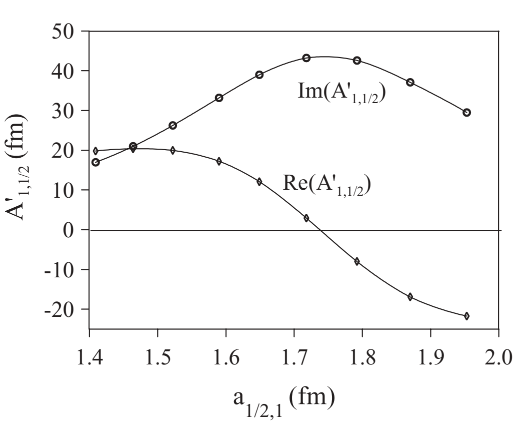

FIG. 3. Real and imaginary parts of the Σd scattering length $A'_{1,1/2}$ as a function of the ΛN $a_{1/2,1}$ scattering length.

The diagram that gives the most important contribution to the width of this state is the one drawn in Fig. 4, since the process $\Sigma N \to \Lambda N$ is dominated by the transition ${}^3S_1 \to {}^3D_1$. For example, at $p_{\mathrm{LAB}}^{\Sigma} = 40$ MeV/c, the on-shell transition potential $V_{\Sigma\Lambda}({}^3S_1 \to {}^3D_1) = 4.542 \times 10^{-2}$ fm^2, while $V_{\Sigma\Lambda}({}^3S_1 \to {}^3S_1) = -1.008 \times 10^{-2}$ fm^2, a factor of 4 smaller. The corresponding on-shell transition amplitudes are $t_{\Sigma\Lambda}({}^3S_1 \to {}^3D_1) = 8.520 \times 10^{-2} + i5.507 \times 10^{-2}$ fm^2, and $t_{\Sigma\Lambda}({}^3S_1 \to {}^3S_1) = -1.061 \times 10^{-2} - i8.961 \times 10^{-3}$ fm^2, roughly a factor of 8 smaller.

We show in Fig. 5 the real part of the Fredholm determinant of the six (I, J) ΣNN channels that are possible for energies below the Σd threshold. The imaginary part of the Fredholm determinant is small and uninteresting. As one can see, the channel (1, 1/2) is the most attractive one, since the Fredholm determinant is close to zero at the Σd threshold, which as mentioned before, indicates the presence of a quasibound state. The next most attractive channel is the $(I, J) = (0, 1/2)$. The ordering of the two attractive ΣNN $J = 1/2$ channels can be easily understood by looking at Table III of Ref. [4]. All the attractive two-body channels in the NN, ΛN, and ΣN subsystems contribute to the $(I, J) = (1, 1/2)$ ΣNN state [the ΣN channels ${}^3S_1(I = 1/2)$ and ${}^1S_0(I = 3/2)$ and the ${}^3S_1(I = 0)$ NN channel], while the $(I, J) = (0, 1/2)$ state does not have contributions from two of them, namely, the ${}^1S_0(I = 3/2)$ ΣN and especially the ${}^3S_1(I = 0)$ NN deuteron channel.

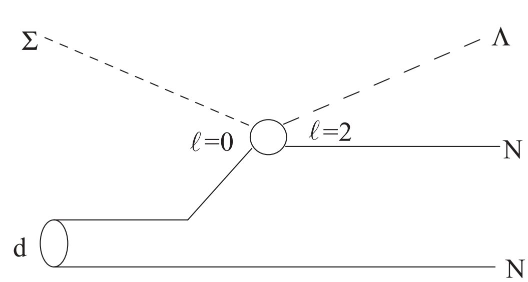

FIG. 4. Diagram that gives the most important contribution to the width of the Σd $(I, J) = (1, 1/2)$ quasibound state.

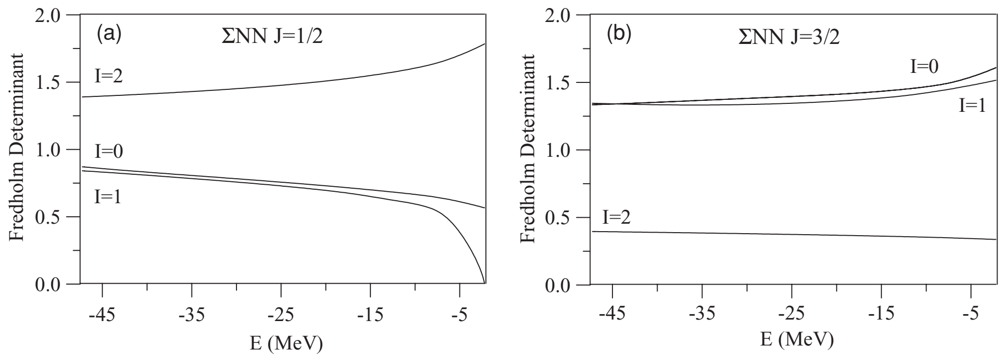

FIG. 5. Fredholm determinant for the (a) $J = 1/2$ and (b) $J = 3/2$ ΣNN channels for the model with $a_{1/2,0} = 2.48$ and $a_{1/2,1} = 1.41$ fm. The Σd continuum starts at $E = -2.225$ MeV, the deuteron binding energy obtained within our model.

IV. SUMMARY

We have solved the Faddeev equations for the ΛNN and ΣNN systems using the hyperon-nucleon and nucleon-nucleon interactions derived from a chiral constituent quark model with full inclusion of the $\Lambda \leftrightarrow \Sigma$ conversion and taking into account all three-body configurations with S and D wave components.

For the ΛNN system, the inclusion of the three-body D wave components increases the attraction, reducing the upper limit of the $a_{1/2,1}$ ΛN scattering length if the $(I, J) = (0, 3/2)$ ΛNN bound state does not exist. This state shows a somewhat larger sensitivity than the hypertriton to the three-body D waves. By including the three-body D wave configurations of all relevant observables of two- and three-baryon systems with strangeness -1, our calculation permits us to constrain the ΛN scattering lengths to $1.41 \leqslant a_{1/2,1} \leqslant 1.58$ fm and $2.33 \leqslant a_{1/2,0} \leqslant 2.48$ fm.

For the ΣNN system, a narrow quasibound state exists near threshold in the $(I, J) = (1, 1/2)$ channel. The width of this state, of the order of 2.1 MeV, comes mainly from the coupling to the ΛNN system in a D wave three-body channel.

The actual interest in two- and three-baryon systems with strangeness -1 [9] makes it worthwhile to pursue the experimental search of narrow peaks near threshold related to the predictions of our model based on the description of almost all known observables of the two- and three-baryons with strangeness -1.

ACKNOWLEDGMENTS

This work was partially funded by Ministerio de Educación y Ciencia under Contract No. FPA2004-05616 and by COFAA-IPN (México).

[1] A. Valcarce, H. Garcilazo, F. Fernández, and P. González, Rep. Prog. Phys. **68**, 965 (2005).
[2] A. Valcarce, H. Garcilazo, and J. Vijande, Phys. Rev. C **72**, 025206 (2005); J. Vijande, F. Fernández, and A. Valcarce, J. Phys. G **31**, 481 (2005).
[3] T. Fernández-Caramés, A. Valcarce, H. Garcilazo, and P. González, Phys. Rev. C **73**, 034004 (2006).
[4] H. Garcilazo, T. Fernández-Caramés, and A. Valcarce, Phys. Rev. C **75**, 034002 (2007).
[5] M. M. Nagels, T. A. Rijken, and J. J. de Swart, Phys. Rev. D **15**, 2547 (1977); U. Straub, Z. Zhang, K. Bräuer, A. Faessler, and S. B. Khadkikar, Nucl. Phys. **A483**, 686 (1988).
[6] G. H. Berthold, H. Zankel, L. Mathelitsch, and H. Garcilazo, Nuovo Cimento A **93**, 89 (1986).
[7] Y. Fujiwara, K. Miyagawa, M. Kohno, and Y. Suzuki, Phys. Rev. C **70**, 024001 (2004).
[8] A. Deloff, Phys. Rev. C **61**, 024004 (2000).
[9] M. Palomba (FINUDA Collaboration), AIP Conf. Proc. **842**, 421 (2006); M. Sato (KEK-PS E471/E549 Collaboration), AIP Conf. Proc. **842**, 480 (2006).